

In vivo longitudinal cellular imaging of small intestine by side-view endomicroscopy

Jinhyo Ahn,¹ Kibaek Choe,¹ Taejun Wang,² Yoonha Hwang,¹ Eunjoo Song,¹
Ki Hean Kim,^{2,3} and Pilhan Kim^{1,*}

¹Graduate School of Nanoscience and Technology (GSNT), Korea Advanced Institute of Science and Technology (KAIST), 291 Deahak-ro, Yuseong-gu, Daejeon, 305-701, South Korea

²Division of Integrative Biosciences and Biotechnology, Pohang University of Science and Technology, San 31, Hyoja-dong, Nam-gu, Pohang, Gyeongbuk 790-784, South Korea

³Department of Mechanical Engineering, Pohang University of Science and Technology, San 31, Hyoja-dong, Nam-gu, Pohang, Gyeongbuk 790-784, South Korea

*pilhan.kim@kaist.ac.kr

Abstract: Visualization of cellular dynamics in the gastrointestinal tract of living mouse model to investigate the pathophysiology has been a long-pursuing goal. Especially, for chronic disease such as Crohn's disease, a longitudinal observation of the luminal surface of the small intestine in the single mouse is highly desirable to investigate the complex pathogenesis in sequential time points. In this work, by utilizing a micro-GRIN lens based side-view endomicroscope integrated into a video-rate confocal microscopy system, we successfully performed minimally-invasive *in vivo* cellular-level visualization of various fluorescent cells and microvasculature in the small intestinal villi. Also, with a transgenic mouse universally expressing photoconvertible protein, Kaede, we demonstrated repetitive cellular-level confocal endoscopic visualization of same area in the small intestinal lumen of a single mouse, which revealed the continuous homeostatic renewal of the small intestinal epithelium.

©2015 Optical Society of America

OCIS codes: (170.2680) Gastrointestinal; (170.2150) Endoscopic imaging; (110.2760) Gradient-index lenses; (170.1790) Confocal microscopy; (170.2520) Fluorescence microscopy.

References and links

1. E. V. Loftus, Jr., "Clinical epidemiology of inflammatory bowel disease: incidence, prevalence, and environmental influences," *Gastroenterology* **126**(6), 1504–1517 (2004).
2. R. J. Xavier and D. K. Podolsky, "Unravelling the pathogenesis of inflammatory bowel disease," *Nature* **448**(7152), 427–434 (2007).
3. G. Bouma and W. Strober, "The immunological and genetic basis of inflammatory bowel disease," *Nat. Rev. Immunol.* **3**(7), 521–533 (2003).
4. M. Gironella, J. L. Iovanna, M. Sans, F. Gil, M. Peñalva, D. Closa, R. Miquel, J. M. Piqué, and J. Panés, "Anti-inflammatory effects of pancreatitis associated protein in inflammatory bowel disease," *Gut* **54**(9), 1244–1253 (2005).
5. S. K. Mazmanian, J. L. Round, and D. L. Kasper, "A microbial symbiosis factor prevents intestinal inflammatory disease," *Nature* **453**(7195), 620–625 (2008).
6. K. Cadwell, K. K. Patel, N. S. Maloney, T. C. Liu, A. C. Ng, C. E. Storer, R. D. Head, R. Xavier, T. S. Stappenbeck, and H. W. Virgin, "Virus-plus-susceptibility gene interaction determines Crohn's disease gene *Atg16L1* phenotypes in intestine," *Cell* **141**(7), 1135–1145 (2010).
7. M. Chieppa, M. Rescigno, A. Y. Huang, and R. N. Germain, "Dynamic imaging of dendritic cell extension into the small bowel lumen in response to epithelial cell TLR engagement," *J. Exp. Med.* **203**(13), 2841–2852 (2006).
8. J. Zhu, B. Lee, K. K. Buhman, and J. X. Cheng, "A dynamic, cytoplasmic triacylglycerol pool in enterocytes revealed by ex vivo and in vivo coherent anti-Stokes Raman scattering imaging," *J. Lipid Res.* **50**(6), 1080–1089 (2009).
9. J. R. McDole, L. W. Wheeler, K. G. McDonald, B. Wang, V. Konjufca, K. A. Knoop, R. D. Newberry, and M. J. Miller, "Goblet cells deliver luminal antigen to CD103+ dendritic cells in the small intestine," *Nature* **483**(7389), 345–349 (2012).
10. S. Foersch, A. Heimann, A. Ayyad, G. A. Spoden, L. Florin, K. Mpoukouvalas, R. Kiesslich, O. Kempster, M. Goetz, and P. Charalampaki, "Confocal laser endomicroscopy for diagnosis and histomorphologic imaging of brain tumors in vivo," *PLoS One* **7**(7), e41760 (2012).

11. S. Foersch, R. Kiesslich, M. J. Waldner, P. Delaney, P. R. Galle, M. F. Neurath, and M. Goetz, "Molecular imaging of VEGF in gastrointestinal cancer *in vivo* using confocal laser endomicroscopy," *Gut* **59**(8), 1046–1055 (2010).
12. D. Moussata, M. Goetz, A. Gloeckner, M. Kerner, B. Campbell, A. Hoffman, S. Biesterfeld, B. Flourie, J. C. Saurin, P. R. Galle, M. F. Neurath, A. J. Watson, and R. Kiesslich, "Confocal laser endomicroscopy is a new imaging modality for recognition of intramucosal bacteria in inflammatory bowel disease *in vivo*," *Gut* **60**(1), 26–33 (2011).
13. D. Kang, R. W. Carruth, M. Kim, S. C. Schlachter, M. Shishkov, K. Woods, N. Tabatabaei, T. Wu, and G. J. Tearney, "Endoscopic probe optics for spectrally encoded confocal microscopy," *Biomed. Opt. Express* **4**(10), 1925–1936 (2013).
14. D. M. Huland, K. Charan, D. G. Ouzounov, J. S. Jones, N. Nishimura, and C. Xu, "Three-photon excited fluorescence imaging of unstained tissue using a GRIN lens endoscope," *Biomed. Opt. Express* **4**(5), 652–658 (2013).
15. G. Oh, S. W. Yoo, Y. Jung, Y. M. Ryu, Y. Park, S. Y. Kim, K. H. Kim, S. Kim, S. J. Myung, and E. Chung, "Intravital imaging of mouse colonic adenoma using MMP-based molecular probes with multi-channel fluorescence endoscopy," *Biomed. Opt. Express* **5**(5), 1677–1689 (2014).
16. J. K. Kim, W. M. Lee, P. Kim, M. Choi, K. Jung, S. Kim, and S. H. Yun, "Fabrication and operation of GRIN probes for *in vivo* fluorescence cellular imaging of internal organs in small animals," *Nat. Protoc.* **7**(8), 1456–1469 (2012).
17. P. Kim, E. Chung, H. Yamashita, K. E. Hung, A. Mizoguchi, R. Kucherlapati, D. Fukumura, R. K. Jain, and S. H. Yun, "In vivo wide-area cellular imaging by side-view endomicroscopy," *Nat. Methods* **7**(4), 303–305 (2010).
18. T. Wang, Q. Li, P. Xiao, J. Ahn, Y. E. Kim, Y. Park, M. Kim, M. Song, E. Chung, W. K. Chung, G. O. Ahn, S. Kim, P. Kim, S. J. Myung, and K. H. Kim, "Gradient index lens based combined two-photon microscopy and optical coherence tomography," *Opt. Express* **22**(11), 12962–12970 (2014).
19. K. Choe, Y. Hwang, H. Seo, and P. Kim, "In vivo high spatiotemporal resolution visualization of circulating T lymphocytes in high endothelial venules of lymph nodes," *J. Biomed. Opt.* **18**(3), 036005 (2013).
20. Y. Hwang, J. Ahn, J. Mun, S. Bae, Y. U. Jeong, N. A. Vinokurov, and P. Kim, "In vivo analysis of THz wave irradiation induced acute inflammatory response in skin by laser-scanning confocal microscopy," *Opt. Express* **22**(10), 11465–11475 (2014).
21. H. Seo, Y. Hwang, K. Choe, and P. Kim, "In vivo image-based quantitation of circulating tumor cells by real-time video-rate confocal microscopy," *Biomed. Opt. Express* **32**(3), 237–238 (2015).
22. I. Choi, H. K. Chung, S. Ramu, H. N. Lee, K. E. Kim, S. Lee, J. Yoo, D. Choi, Y. S. Lee, B. Aguilar, and Y. K. Hong, "Visualization of lymphatic vessels by Prox1-promoter directed GFP reporter in a bacterial artificial chromosome-based transgenic mouse," *Blood* **117**(1), 362–365 (2011).
23. M. Tomura, N. Yoshida, J. Tanaka, S. Karasawa, Y. Miwa, A. Miyawaki, and O. Kanagawa, "Monitoring cellular movement *in vivo* with photoconvertible fluorescence protein "Kaede" transgenic mice," *Proc. Natl. Acad. Sci. U.S.A.* **105**(31), 10871–10876 (2008).
24. R. Ando, H. Hama, M. Yamamoto-Hino, H. Mizuno, and A. Miyawaki, "An optical marker based on the UV-induced green-to-red photoconversion of a fluorescent protein," *Proc. Natl. Acad. Sci. U.S.A.* **99**(20), 12651–12656 (2002).
25. C. Varol, E. Zigmund, and S. Jung, "Securing the immune tightrope: mononuclear phagocytes in the intestinal lamina propria," *Nat. Rev. Immunol.* **10**(6), 415–426 (2010).
26. M. Latta, K. Mohan, and T. B. Issekutz, "CXCR6 is expressed on T cells in both T helper type 1 (Th1) inflammation and allergen-induced Th2 lung inflammation but is only a weak mediator of chemotaxis," *Immunology* **121**(4), 555–564 (2007).
27. N. Barker, "Adult intestinal stem cells: critical drivers of epithelial homeostasis and regeneration," *Nat. Rev. Mol. Cell Biol.* **15**(1), 19–33 (2013).
28. H. Tian, B. Biehs, S. Warming, K. G. Leong, L. Rangell, O. D. Klein, and F. J. de Sauvage, "A reserve stem cell population in small intestine renders Lgr5-positive cells dispensable," *Nature* **478**(7368), 255–259 (2011).
29. A. Merlos-Suárez, F. M. Barriga, P. Jung, M. Iglesias, M. V. Céspedes, D. Rossell, M. Sevillano, X. Hernando-Mombalona, V. da Silva-Diz, P. Muñoz, H. Clevers, E. Sancho, R. Manges, and E. Battle, "The intestinal stem cell signature identifies colorectal cancer stem cells and predicts disease relapse," *Cell Stem Cell* **8**(5), 511–524 (2011).

1. Introduction

For inflammatory bowel disease research, direct observation of cellular phenomena in the gastrointestinal tract of a model mouse has been a long-pursuing goal. Especially, for chronic condition such as Crohn's disease mostly affecting small intestine, longitudinal and repetitive cellular visualization and analysis of luminal surfaces under the natural *in vivo* environment is highly desirable as it can provide valuable information for investigating complex pathogenesis in sequential viewpoint [1–3]. To analyze the cellular-level pathologies in inflammatory bowel disease, most previous studies have been primarily dependent on *ex vivo* histological observation of excised intestinal tissues [4–6]. However, it could provide only static information at a single specific time point of excision, which gave significant limitations in

investigating dynamic longitudinal events in the intestinal tract such as stromal cell-cell interaction, immune cell trafficking and cellular-level remodeling [2].

During the last decade, laser-scanning fluorescence microscopy such as confocal and two-photon microscopy has been actively utilized to visualize dynamic pathophysiological cellular processes in various animal models for human diseases. However, *in vivo* applications of these high-resolution microscopy techniques to live animal model have been mostly limited to easily accessible tissues such as skin, eye or some tissues exposable by simple surgical procedure. Although not impossible, intestinal tracts those are difficult to exteriorize and access with conventional large-sized imaging optics have been remained as a particularly challenging tissue to be visualized in microscopic cellular resolution *in vivo*. Notably, there are a few reports demonstrated the dynamic cellular-level imaging of small intestine of live mouse model by high-resolution laser-scanning microscopy [7–9]. However, all of these reports relied on intensive surgical procedures to exteriorize small intestine and secure an enough space to apply large-sized imaging objective lens, which is too invasive to be repeated on a single animal. To achieve longitudinal and repetitive cellular visualization and analysis of luminal surfaces of small intestinal tract under the natural *in vivo* environment, a significantly less invasive approach is clearly required.

Endomicroscopy have been actively developed for minimally invasive visualization of internal organs of small animal models [10–17]. High-resolution confocal endomicroscopy relying on resonant single-mode fiber scanning has successfully visualized brain tumor in rat model [10], surgically exposed colorectal cancer [11] and infected small intestine [12] in mouse model, demonstrating its potential for a cellular-level diagnostic tool. Although it is only demonstrated by using *ex vivo* tissue, spectrally encoded confocal microscopy [13] and three-photon microscopy [14] equipped with custom designed endoscopic probes have successfully obtained cellular-level images from swine esophagus and mouse lung respectively without any exogenous labeling, validating their clinical applicability. A commercial rigid endoscope modified for fluorescence imaging has applied to obtain a fish-eye view image of colorectal cancer in mouse model *in vivo* [15]. Side-view confocal endomicroscopy [16, 17] based on miniature GRIN lens and micro-prism has successfully demonstrated a repetitive cellular-level imaging of colorectal cancer development in mouse model. However, in contrast to the colon which is easily accessible through a natural orifice; anus, longitudinal repetitive cellular-level visualization of same area in the small intestine has not yet been achieved.

In this work, by utilizing a micro-GRIN lens based side-view endomicroscope integrated into a video-rate confocal microscopy system, we performed minimally-invasive cellular-level visualization of microvasculature and fluorescent cells in the small intestine, *in vivo*. The side-view endomicroscope was fabricated by stacking 2 mm diameter GRIN lenses – a coupling lens, a relay lens with 1 pitch and a high NA imaging lens attached with an aluminum coated 90° micro-prism (1.3 mm of base length). To minimize the invasiveness of the imaging procedure, the side-view endomicroscope was carefully inserted into the lumen of small intestine via a small incision on the abdominal skin, peritoneum and a needle hole on the wall of small intestine. By using various transgenic mice expressing green fluorescent protein (GFP), we successfully visualized the distribution of mononuclear phagocytes (CX₃CR1-GFP), T cells (CXCR6-GFP) and lymphatic vessel (Prox1-GFP) along with microvasculature in the small intestinal villi, *in vivo*. Also, fluorescently labeled red blood cells (RBC) those were rapidly flowing through the capillary network in the small intestinal villi were directly imaged in real time. Finally, by using a transgenic mouse universally expressing photoconvertible protein, Kaede, we demonstrated repetitive cellular-level visualization of same area in the small intestinal lumen of the single mouse, revealing the continuous self-renewal of the small intestinal epithelium *in vivo*.

2. Materials and methods

2.1 GRIN lens based side-view endomicroscope

Gradient-index (GRIN) optics plays a role as an alternative way to guide an optical beam by gradual variation of the refractive index of a lens. In contrast to a conventional lens which has different refractive index only at the interface between materials, a GRIN lens depends on a gradual refractive index change within the material. The GRIN lens has several unique advantages for implementation in a miniaturized optical device. A flat surface in cylindrical shapes simplifies the fabrication process to assemble multiple GRIN lenses into a single device with a desired performance. Also GRIN lens can achieve a relatively high NA with a very small optical aperture of several millimeters, which makes the GRIN lens as a preferred choice to fabricate a miniaturized optical device for visualization of microscopic object. In this work, the previously reported micro-GRIN lens based side-view endomicroscope [18]

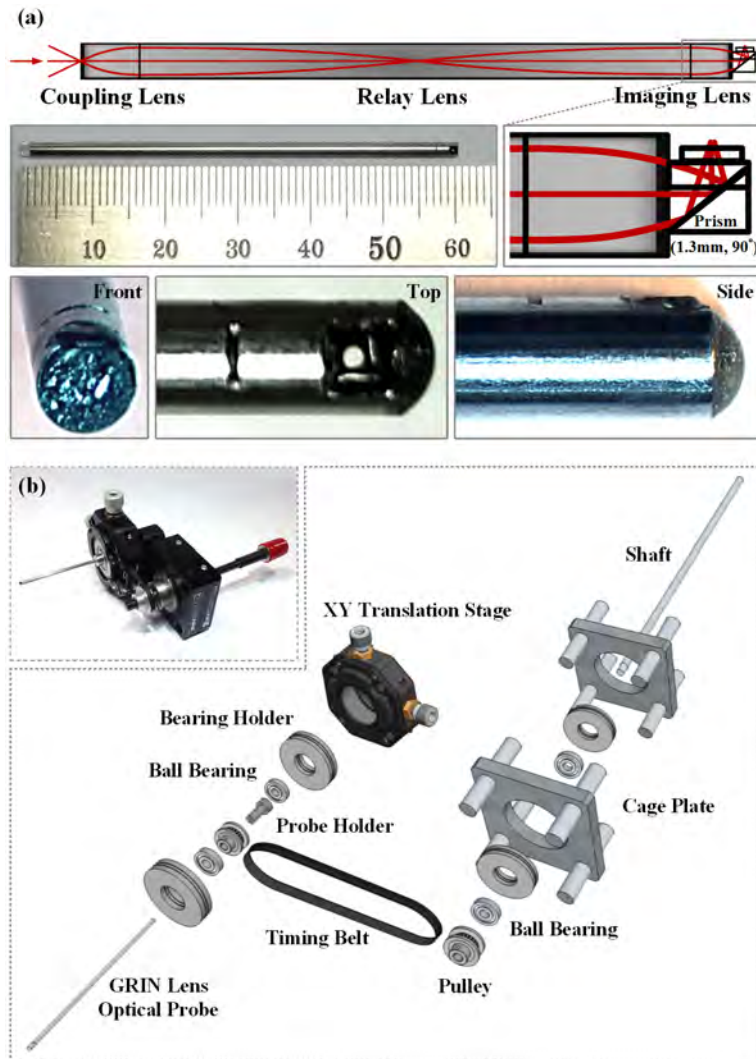


Fig. 1. (a) Schematic and magnified photos of the fabricated side-view endomicroscope incorporating three GRIN lenses (coupling, relay and imaging lens) and an aluminum coated 90° microprism. (b) Schematic and a photo of the custom-built 360° rotation mount for the side-view endomicroscope.

was utilized. The endoscopic probe was fabricated by GRINTECH with a custom designed GRIN lens. It consists of a high NA coupling lens (NA 0.5, IFRL-200-023-50-NC), a relay lens with 1 pitch (NA 0.1, IFRL-200-100-11-NC) and a imaging lens (NA 0.5, IFRL-200-cust-50-NC) with an aluminum coated micro prism (1.3 mm in length) attached to reflect the transmitted light for side-viewing. Figure 1(a) shows the schematic and magnified photos of the fabricated side-view endomicroscope. The fabricated optical components were packaged in a stainless-steel tube to have a diameter of 2.2 mm and length of 60 mm. The inner diameter of mouse small intestinal tract is approximately 2 mm which is slightly smaller than the diameter of the side-view endomicroscope, 2.2 mm. Therefore the small intestine wraps the probe smoothly with small tension. It makes the luminal wall of small intestine keep a uniform contact with the side-view endomicroscope in all 360 degree, which helps to achieve better image quality while navigating through the small intestine with the rotating side-view endomicroscope. At the distal surface of the micro-prism, a cover slip was attached by topical application of UV-curing optical adhesive (NOA81, Thorlabs). Additionally, to avoid potential damage to the luminal wall of small intestine, the entire distal end of the probe was finished in round shape with a UV-curing optical adhesive as shown in the photograph of Fig. 1(a). As shown in Fig. 1(b), the fully-packaged side-view endomicroscope was then inserted into the through hole of probe holder fixed to a pulley and two ball bearings (FL6700ZZ, Misumi). Then it was mounted to the X-Y translation stage (CXY1, Thorlabs) for the precise adjustment of the probe position. The focal plane was formed roughly at the surface of the probe and was continuously adjustable in range of 250 μm . Focal plane in z-axis was adjustable by changing the distance between the objective lens (LUCPlanFLN 40X, NA 0.6, Olympus) and the proximal end of the endomicroscope which is supported by X-Y translation stage and Z-axis translation stage (9061-COM-M, Newport). The endomicroscope could be endlessly rotated in 360° by a shaft (SFMR5-100, Misumi) fixed to a pulley connected to the other probe-holding pulley by a timing belt. After the integration into the imaging system, the side-view endomicroscope provides the circular-shaped field of view (FOV) of 311 μm in diameter with 10 μm axial resolution.

2.2 Video-rate laser-scanning confocal microscope system

The side-view endomicroscope was integrated to a custom-built video-rate laser scanning confocal microscope system implemented by modifying the previously developed imaging system [19–21]. Figure 2 shows the schematic and the photos of the microscope system equipped with the side-view endoscope for *in vivo* small intestine imaging. Four continuous-wave laser modules at 405 nm (Coherent OBIS), 488 nm (Cobolt MLD), 561 nm (Cobolt Jive) and 640 nm (Cobolt MLD) were used as excitation sources for multi-color fluorescence imaging. All the laser beams were combined by dichroic beam splitters (DBS1, FF593-Di03; DBS2, Di01-R405; DBS3, FF520-Di02, Semrock) and delivered to a multi-edge dichroic beam splitter (DBS4, Di01-R405/488/561/635, Semrock). The aligned laser beams were raster-scanned by a rotating 36 facet polygonal mirror (MC-5, Lincoln Laser) for fast X-axis scanning at 17.28 kHz and a galvanometer mirror scanner (6230H, Cambridge Technology) for slow Y-axis scanning at 30 Hz. The raster-scanning laser beam was delivered to the back aperture of objective lens. Relaying lenses were selected to achieve the field of view (FOV) of 250 \times 250 μm with 40X objective lenses (LUCPlanFLN, NA 0.6, Olympus). The scanning laser beam was delivered to the tissues of internal organs of an anesthetized mouse on a XYZ translation stage through the side-view endomicroscope. The fluorescence signals from the sample were epi-detected by the objective lens, back propagated through the scanning optics and then separated by the multi-edge dichroic beam splitter, DBS4. Subsequently, the fluorescence signals were split into four single-color signals by dichroic beam splitters (DBS5, FF484-Di01; DBS6, FF560-Di01; DBS7, FF649-Di01, Semrock) and band pass filters (BPF1, FF01-442/46; BPF2, FF02-525/50; BPF3, FF01-600/37; BPF4, FF01-685/40, Semrock) and simultaneously detected by four photomultiplier tubes (PMT; R9110, Hamamatsu). The electronic outputs from the PMTs were digitized by a frame grabber (Solios, Matrox) with a sampling rate of 10 MHz for each channel. The images of 512 \times 512

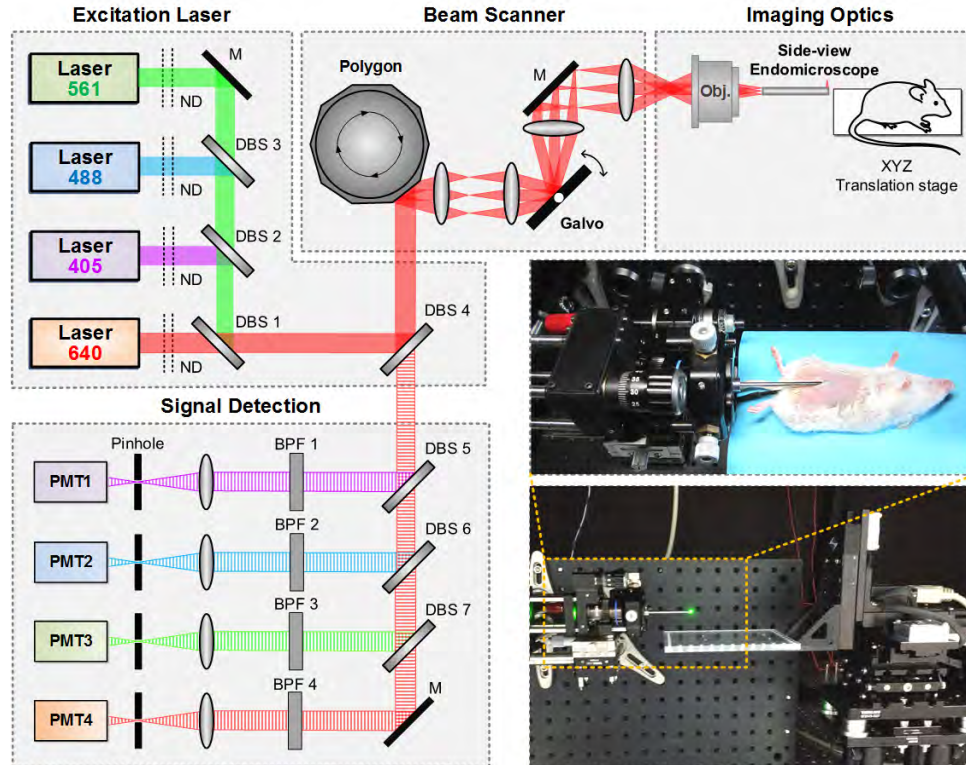


Fig. 2. Schematic and photo of a custom-built laser scanning confocal microscopy system integrated with side-view endomicroscope: ND, neutral density filter; DBS, dichroic beam splitter; BPF, band pass filter; M, mirror; PMT, photomultiplier tube; Obj, objective lens.

pixels were displayed and recorded in real time at a frame rate of 30 Hz by custom-written imaging software using Visual C++ and Matrox Imaging Library (MIL9, Matrox).

2.3 Animal

In this study, CX₃CR1-GFP, CXCR6-GFP (Stock no. 005582, 005693 Jackson Laboratory) and Prox1-GFP mice (kindly provided by Dr. Hong [22]) which exclusively express GFP on mononuclear phagocytes, helper T-cells and lymphatic vessels in the small intestine, respectively, were used to demonstrate the capability of the side-view endomicroscope for *in vivo* cellular-level visualization of small intestine. Kaede transgenic mice (kindly provided by Dr. Tomura and Dr. Miwa [23]) which universally express a photo-convertible fluorescent protein 'Kaede', were used to longitudinally visualize the regenerated epithelium of small intestinal villi. Kaede protein undergoes irreversible photoconversion from green to red fluorescent emission in response to UV-violet light [24].

2.4 Imaging procedure

For the *in vivo* imaging, mouse was anesthetized by intraperitoneal injection of a mixture of zoletil (30 mg/kg) and xylazine (10 mg/kg). Mouse body temperature was maintained at 36°C by a temperature monitoring and homeothermic control system (RightTemp, Kent Scientific). The mouse skin was shaved by a hair clippers and removal cream before surgical procedure for the imaging. To visualize the microvasculature in the small intestinal villi, anti-CD31 antibody (Stock no. 553708, BD Biosciences) conjugated with a far-red color fluorophore, AlexaFluor 647 (A20006, Invitrogen), was intravenously injected into the mouse at 3 hours before the imaging. To visualize the rapidly flowing red blood cells (RBC) in the capillary of the small intestinal villi, FITC-dextran (BCBF2730V, Sigma) as a fluorescent angiography

agent and fluorescently labeled RBCs by DiD (V-22889, Invitrogen) were intravenously injected.

After a small incision on the abdominal skin and peritoneum of the anesthetized mouse, the endomicroscope was carefully inserted through a 2 mm diameter hole made on intestinal wall by a needle into the lumen of small intestine. Before the insertion of the endomicroscope, 50 μ l of PBS was administrated into the lumen as a lubricant to reduce the friction between the probe and luminal wall of small intestine. After imaging, small intestinal wall, peritoneum and skin were independently closed by a surgical suture. For longitudinal observation of a single mouse, repetitive surgical procedure including the incision and suture of the abdomen and the small intestinal wall was conducted with two day interval at the same location of the anesthetized mouse. Also, anti-inflammatory drugs including trimethoprim and sulfamethoxazole were supplied into the drinking water and a non-steroidal anti-inflammatory drug, Rimadyl, was administrated by intraperitoneal injection every day.

3. Results

3.1 *In vivo* cellular-level visualization of the small intestine by side-view endomicroscope

The inner luminal surface of the small intestine has numerous villi those are covered by a single layer of epithelial cells, enterocytes. A loose connective tissue under the epithelium, called lamina propria, accommodates numerous immune cells, blood capillaries and lymphatic vessel. As shown in Fig. 3(a)-3(c), we successfully obtained *in vivo* cellular-level images of individual cells and microvasculature from the small intestine of anesthetized transgenic mice expressing the GFP in various cells. Mononuclear phagocytes (CX₃CR1-GFP [25]), T-cells (CXCR6-GFP [26]) and lymphatic vessels (Prox1-GFP [22]) existing in the lamina propria of each villus were clearly visualized *in vivo* by using the side-view endomicroscope as shown in Fig. 3(a), 3(b) and 3(c), respectively. Capillary vessels fluorescently labeled by the intravenous injection of anti-CD31 antibody conjugated with far-red fluorophore AlexaFluor 647 were simultaneously imaged *in vivo*. As shown in Fig. 3(a), CX₃CR1⁺ mononuclear phagocytes were densely populated in the lamina propria and mostly located at perivascular space. T-cells were also mostly located at perivascular space as shown in Fig. 3(b). The lymphatic vessel located at the center of each villus, called lacteal, and the nuclei of lymphatic endothelial cells strongly expressing Prox-1 are clearly visible in Fig. 3(c). In addition, by utilizing the video-rate image acquisition capability of the imaging system, we successfully captured images of rapidly flowing red blood cells (RBC) in the capillary blood vessels of small intestine as shown in Fig. 3(d) by using the side-view endomicroscope. 2MDa FITC-dextran was intravenously injected as a fluorescent angiography agent to label the blood plasma of capillary vessels. RBCs labeled by far-red fluorophore, DiD, were also intravenously injected to wildtype C57BL/6 mouse. In the Fig. 3(d) shows the individual image frames obtained in 30 frames per second. Rapidly flowing RBCs (white arrowhead) in the capillary blood vessels in the villus of small intestine were clearly visualized.

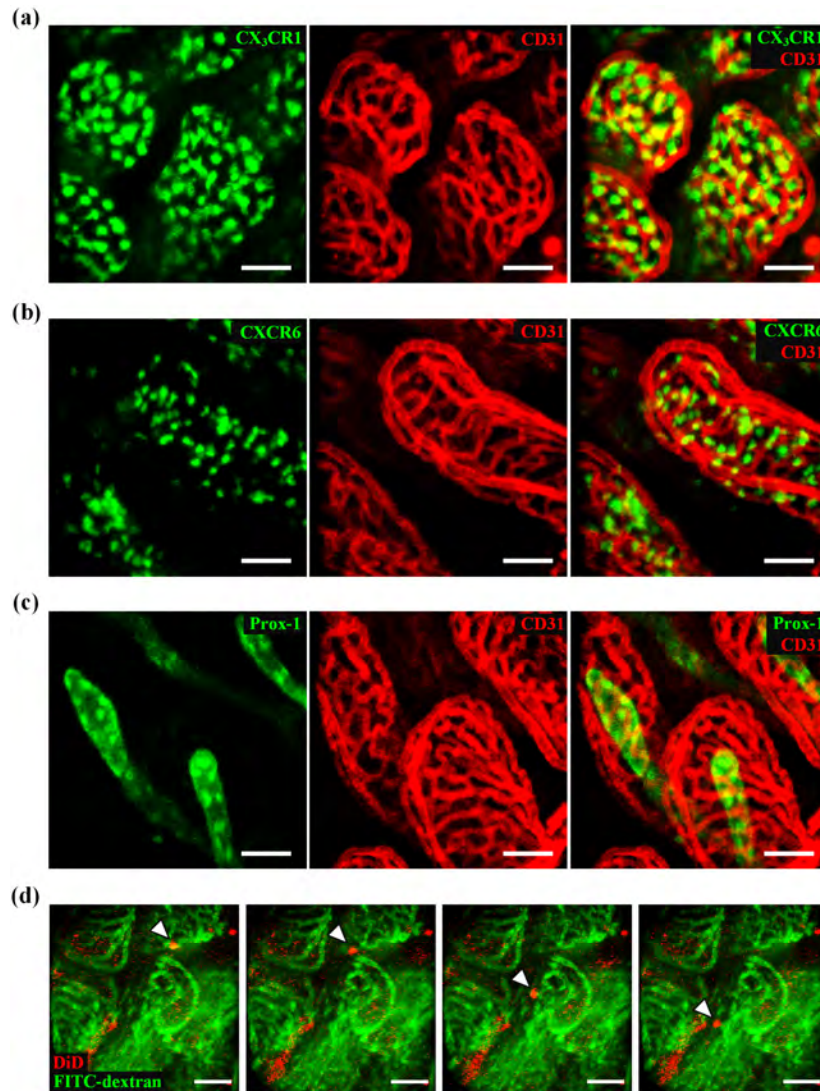


Fig. 3. Representative *in vivo* images obtained from the small intestine of (a) CX₃CR1-GFP mouse, (b) CXCR6-GFP mouse, and (c) Prox1-GFP mouse, respectively, along with capillary blood vessels (red) by using side-view endomicroscope. (d) Real-time fluorescence images of circulating red blood cell (red, white arrowhead) in the blood vessel (green) of the villi. Time interval: 1 sec. Scale bar: 50 μ m.

3.2 Longitudinal repetitive imaging of the small intestine by side-view endomicroscope

Due to persistent aggression of food contents and pathogenic factors, the inner epithelium of the small intestine suffers from very high rate cell death [27]. Thus the epithelial cells of the villi are required to renew themselves quickly. Enterocytes, the most abundant type of cells in the epithelium of the villi, are replaced in every 3~5 days by the newly differentiated cells those were originated from the stem cells existing in the crypt bases [28, 29]. The newly generated cells from the crypt continuously migrate toward the epithelial tip of the villi and replace the dead cell. We successfully visualized the epithelial cell renewal at the small intestinal villi by performing repetitive longitudinal cellular-level *in vivo* visualization of same area in the small intestine in the single mouse with the side-view endomicroscope. To distinguish the pre-existing epithelial cells undergoing continuous cell death from the newly

migrated cells replacing them, we used a transgenic mouse universally expressing photoconvertible protein, Kaede [23, 24]. Under the ultraviolet light (350 – 400 nm) irradiation, Kaede irreversibly transmutes its fluorescent emission from green (peak wavelength: 518 nm) to red (peak wavelength: 582 nm). Photoconverted Kaede expressing cell retains the red fluorescence, while all of newly generated cell expresses original green-fluorescent Kaede. Therefore, once we photoconverted the epithelial cells in the small intestine of a Kaede mouse, we could clearly identify the newly generated epithelial cells migrated from the crypt base by their green fluorescence. Furthermore, we could also repetitively find the exactly same area of the small intestine with relatively small FOV of the side-view endomicroscope by simply searching the photoconverted area which is clearly distinguishable from neighborhood area.

Figure 4 shows longitudinal repetitive cellular-level visualization of the same area in the small intestine of the Kaede mouse with 2 days interval. At day 0, we first identified the normal-looking area in the small intestine and then delivered the 405nm light through the side-view endomicroscope to irreversibly photoconvert the Kaede protein inside the villi. The optical power of 405 nm delivered to the tissue was measured to be 480 μ W and the irradiation time was 10 seconds. We used 488 nm and 561 nm laser light to excite the green-fluorescent Kaede and photoconverted red-fluorescent Kaede, respectively. Green- and red-fluorescent Kaede were detected through the bandpass filter transmitting 500 - 550nm and 581.5 - 618.5nm, respectively. As shown in Fig. 4, after the delivery of the 405nm light, all of the epithelial cells and residing cells in the lamina propria of the villi were completely photoconverted to red-fluorescent. After 2 days, we could observe newly migrated green-fluorescent Kaede expressing cells in the lamina propria (arrow) those were immune cells actively circulating the whole body for immune surveillance. In contrast, epithelial cells, mostly enterocytes (arrowhead), still retained red-fluorescent Kaede, suggesting that the renewal was not yet occurred. To note, we observed colocalization of green and red fluorescence signals from the newly migrated green-fluorescent Kaede cells, which was caused by the fluorescence bleed-through from green- to red-fluorescence detection channel (star). After 4 days, we could observe the most of enterocytes (arrowhead) express original green-fluorescent Kaede, suggesting the renewal of the epithelium of the small intestinal villi.

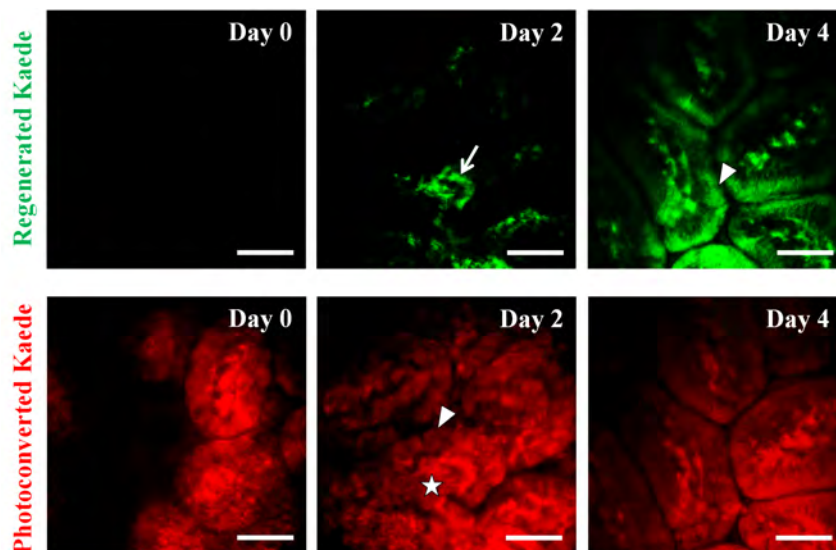


Fig. 4. Longitudinal repetitive visualization of same area in the small intestine of the single Kaede mouse obtained by side-view endomicroscope in 2 days interval. Lamina propria residing cells (arrow) and enterocytes (arrowhead) were longitudinally monitored. Scale bar: 50 μ m.

4. Conclusion

In this work, we achieved minimally-invasive cellular-level *in vivo* visualization of microvasculature and fluorescent cells in the small intestine by utilizing a micro-GRIN lens based side-view endomicroscope, which enabled a repetitive imaging in a single mouse. By using various transgenic GFP reporter mice, we successfully acquired the images of mononuclear phagocytes (CX₃CR1-GFP), T cells (CXCR6-GFP) and lymphatic vessel (Prox1-GFP) along with microvasculature in the small intestinal villi, *in vivo*. Most importantly, by using a transgenic mouse expressing photoconvertible protein, Kaede, we achieved repetitive cellular-level visualization of same area in the small intestinal lumen of a single mouse, revealing the continuous self-renewal of the small intestinal epithelium *in vivo*. By being applied to various mouse models for Crohn's disease and ulcerative colitis, this technique can provide a new insight to understand complex pathophysiology of these diseases originated from the epithelium of intestinal tracts.

Acknowledgments

This work was supported by the World Class Institute program (WCI 2011-001), the Engineering Research Center program (NRF-2009-0083512), the Global Frontier Project (CAMM-2014M3A6B3063705) of National Research Foundation of Korea and the Converging Research Center Program (2011K000864) funded by the Ministry of Science, ICT and Future Planning, Republic of Korea and the Korea Healthcare Technology R&D Project funded by Ministry of Health and Welfare, Republic of Korea (HN12C0063, HI13C2181).